

Transport Simulation of Internal Transport Barrier Formation Using Various Neoclassical Transport Models

HONDA Mitsuru, FUKUYAMA Atsushi and YAGI Masatoshi¹

Department of Nuclear Engineering, Kyoto University, Kyoto 606-8501, Japan

¹*Research Institute for Applied Mechanics, Kyushu University, Kasuga 816-8580, Japan*

(Received: 9 December 2003 / Accepted: 7 April 2004)

Abstract

TASK/TR is a diffusive transport code based on the current diffusive ballooning mode model and has successfully reproduced an internal transport barrier (ITB) in the high β_p mode and in the reversed shear configuration. Using this code, we have examined the difference of various neoclassical transport models and the effect on the behavior of the ITB.

Keywords:

internal transport barrier (ITB), current diffusive ballooning mode (CDBM), neoclassical transport, bootstrap current, thermal diffusivity, neoclassical plasma resistivity

1. Introduction

The formation of an internal transport barrier (ITB) has been observed in various operation conditions on major tokamaks. The observation of improved core plasma confinement has facilitated the study of the mechanism of the ITB formation. One of the theory-based transport model [1] developed is the current diffusive ballooning mode (CDBM) model which is derived from the self-sustained turbulence theory and successfully described the formation of the ITB in high β_p plasmas and in the reversed magnetic shear configuration [2]. This model predicts the reduction of the thermal diffusivity χ_{CDBM} where the magnetic shear s is weak or negative and the normalized pressure gradient α becomes large. On the other hand, various neoclassical models of the bootstrap current have been developed. Since the bootstrap current plays a significant role in forming the ITB and has the possibility to allow us to achieve a long-time operation in tokamaks, it is important to understand the behavior of the models in tokamak simulation. We have implemented those models such as NCLASS [3], the approximate formulas by Sauter [4] and Hinton & Hazeltine model [5] into the one-dimensional transport code, TASK/TR, and we examine the difference of the profiles amongst these models in the case of the ITB.

2. Diffusive transport code, TASK/TR

We solve the transport equations as follows:

$$\begin{aligned} \frac{\partial}{\partial t} (n_s V') = & \\ & - \frac{\partial}{\partial \rho} \left(V' \langle |\nabla \rho| \rangle n_s V_s - V' \langle |\nabla \rho|^2 \rangle D_s \frac{\partial n_s}{\partial \rho} \right) \\ & + S_s V' \end{aligned} \quad (1)$$

$$\begin{aligned} \frac{\partial}{\partial t} \left(\frac{3}{2} n_s T_s V'^{5/3} \right) = & \\ & - V'^{2/3} \frac{\partial}{\partial \rho} \left(V' \langle |\nabla \rho| \rangle \frac{3}{2} n_s T_s V_{Es} \right. \\ & \left. - V' \langle |\nabla \rho|^2 \rangle \frac{3}{2} D_s T_s \frac{\partial n_s}{\partial \rho} \right. \\ & \left. - V' \langle |\nabla \rho|^2 \rangle n_s \chi_s \frac{\partial n_s}{\partial \rho} \right) + S_{Es} V'^{5/3} \end{aligned} \quad (2)$$

$$\begin{aligned} \frac{\partial B_\theta}{\partial t} = \frac{\partial}{\partial \rho} \left[\frac{\eta_{\parallel}}{\mu_0} \frac{F}{V' \langle R^{-2} \rangle} \frac{\partial}{\partial \rho} \left(\frac{V'}{F} \langle \frac{|\nabla \rho|^2}{R^2} \rangle B_\theta \right) \right. \\ \left. - \frac{\eta_{\parallel}}{FR_0} \langle \frac{|\nabla \rho|}{R^{-2}} \rangle \langle (J_{CD} + J_{BS}) B \rangle \right] \end{aligned} \quad (3)$$

where V is the plasma volume, ρ is the normalized minor radius, $V' = dV/d\rho$, $V_{Es} = V_{Ks} + (3/2)V_s$, V_{Ks} is the heat pinch,

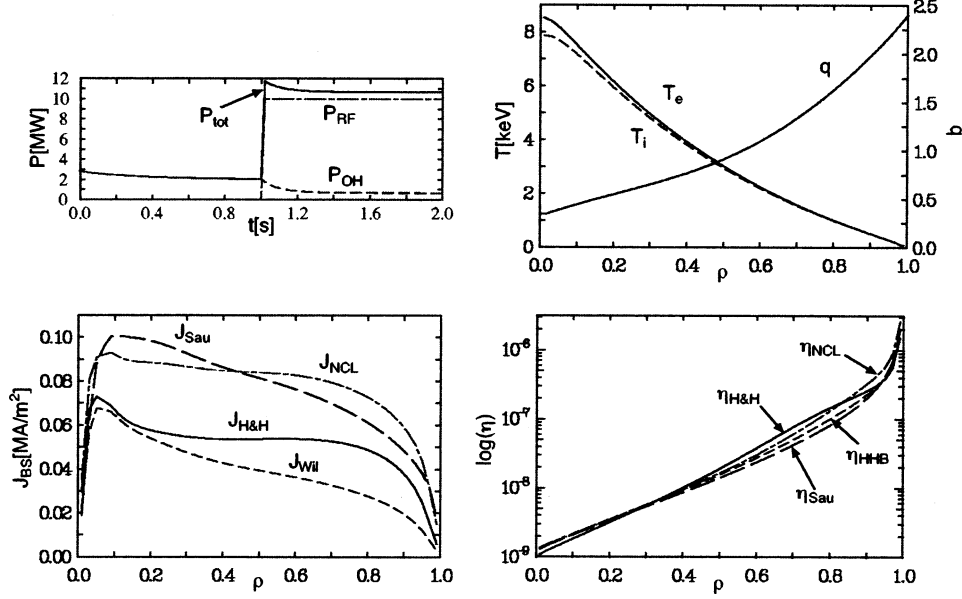


Fig. 1 Time dependence, temperature and q profiles, bootstrap current profile and logarithmic scale profile of neoclassical resistivity with NCLASS as typical neoclassical model in the L mode.

V_s is the particle pinch, $F = RB_\phi$, $\langle \rangle$ represents a magnetic surface average, S_s and S_{Es} are the source terms, and a subscript s denotes particle species. Other notations are standard.

The CDBM transport model [2] includes the effects of $E \times B$ shear stabilization. In this paper, however, we neglect it for simplicity.

We have carried out tokamak transport simulations using the thermal diffusivity derived from the CDBM model

$$\chi_{CDBM} = CF(s, \alpha, \kappa_m) \alpha^{3/2} \frac{c^2}{\omega_{pe}^2} \frac{v_A}{qR} \quad (4)$$

where the normalized pressure gradient $\alpha \equiv -q^2 R (d\beta/dr)$, magnetic shear $s \equiv (r/q)(dq/dr)$, magnetic curvature $\kappa_m \equiv -(r/R)(1 - 1/q^2)$. The factor $F(s, \alpha, \kappa_m)$ represents the reduction due to weak or negative magnetic shear and large Shafranov shift. The explicit expression of F is given in Ref. [2]. The coefficient C is adjusted that the confinement time is consistent with the ITER89-P L mode scaling for typical plasma parameters. The present CDBM model does not distinguish the thermal diffusivities of electrons and ions. The transport coefficients are expressed as a sum of the neoclassical contribution χ_{NC} and the anomalous contribution χ_{CDBM} . Therefore, the thermal diffusivity of the electron and ion are:

$$\chi_e = \chi_{NC,e} + \chi_{CDBM} \quad (5)$$

$$\chi_i = \chi_{NC,i} + \chi_{CDBM} \quad (6)$$

In this paper, the above coefficient C is set to be 12.

3. In the case of the L mode

In order to clarify the difference amongst the bootstrap current models, we set up the typical L mode profiles by

assuming a certain model and starting from given initial profiles. Then we calculate the bootstrap current density and the resistivity profiles with various neoclassical models. The equation of continuity is not calculated because we focus on a thermal transport and make the difference of the models clearer.

We use the following plasma parameters, $R = 3$ m, $a = 1.2$ m, $\kappa = 1$, $B = 3$ T, $I_p = 3$ MA, $n_e(0) = 0.5 \times 10^{20} \text{ m}^{-3}$ and $T_e(0) = T_i(0) = 1.5$ keV. In addition we select NCLASS to calculate the profile. In this calculation, on-axis heating of 10 MW is switched on at $t = 1$ s, and the profiles at $t = 2$ s are compared. In Fig. 1, we make a comparison amongst the Wilson model [6], the Hinton and Hazeltine model [5], the Sauter model [4] and NCLASS [3] in terms of the bootstrap current and the neoclassical resistivity in the L mode. As the neoclassical resistivity, we use the Hinton and Hazeltine model, the Hirshman, Hawryluk and Birge model [7], the Sauter model and NCLASS.

All the logarithmic profiles of the neoclassical resistivity are rather good agreement, while the profile of the bootstrap current are not. The radial dependence of J_{Sau} is similar with that of J_{Wil} while the magnitude of J_{Sau} is twice as much as that of J_{Wil} . We can also find a similar tendency between J_{NCL} and $J_{H\&H}$.

4. In the case of the high β_p mode

Now we consider in the high β_p mode. The plasma parameters and initial conditions are the same as those of L mode except $\kappa = 1.5$ and $I_p = 1$ MA. Since I_p is lower than the previous case, the poloidal beta becomes as high as unity and the bootstrap current is strongly enhanced.

Figure 2 indicates that all the bootstrap current profiles have similar shapes, but their magnitudes are significantly

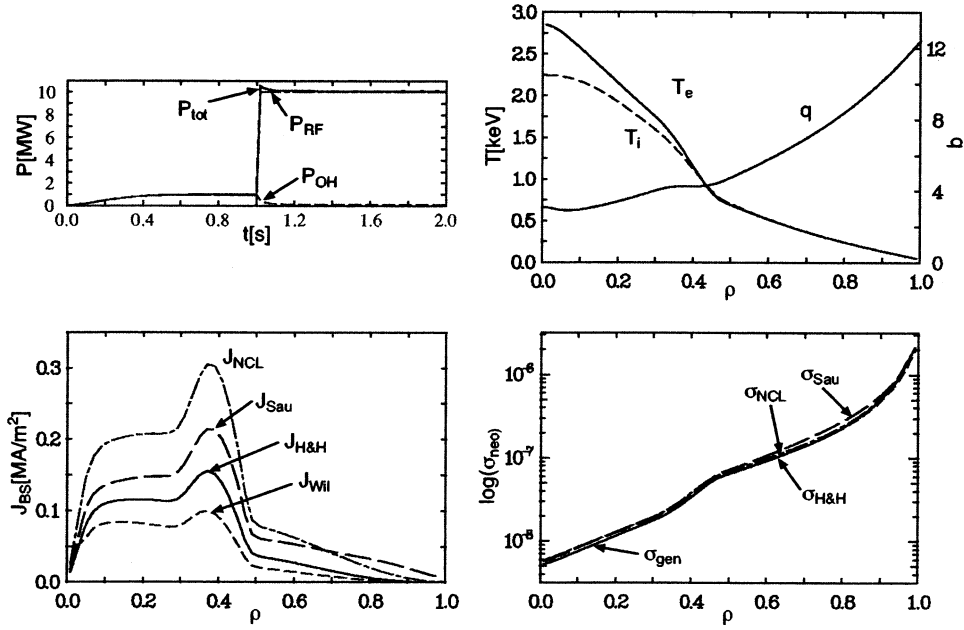


Fig. 2 Time dependence, temperature and q profiles, bootstrap current profile and logarithmic scale profile of neoclassical resistivity with NCLASS as typical neoclassical model in high β_p mode.

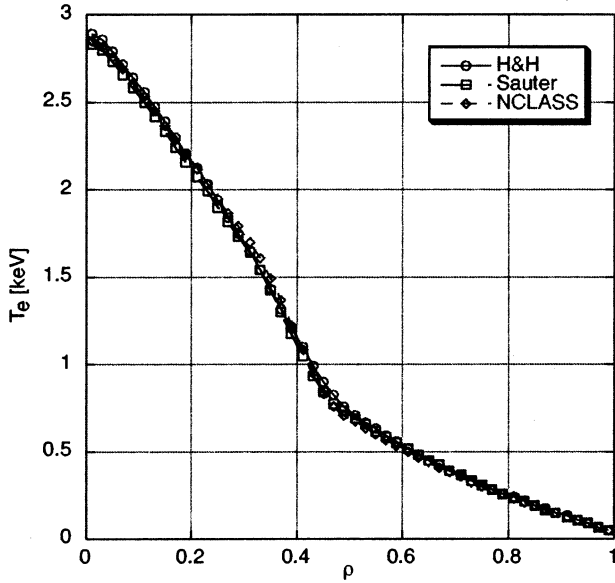


Fig. 3 (a): Electron temperature profile in the high β_p mode at $t = 2$ s.

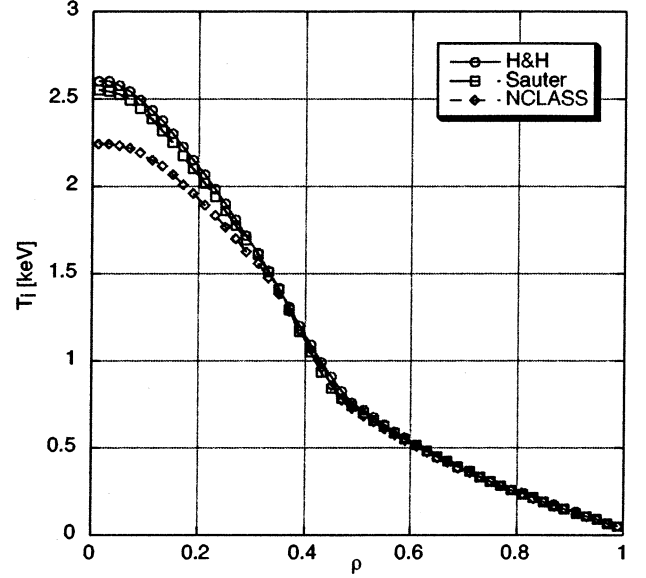


Fig. 3 (b): Ion temperature profile in the high β_p mode at $t = 2$ s.

different. The elongation κ contributes to enhance the difference. That is because we have not rigorously included the elongation effect in the calculation of the poloidal magnetic field β_p comprised in the formulas of J_{Sau} , $J_{H\&H}$ and J_{Wii} .

In order to investigate the difference of the ITB formation, we have carried out a transport simulation on each model with the same time sequence with those in Fig. 2. We show electron/ion temperature profiles at $t = 2$ s in Fig. 3. We have quite a good agreement in the electron temperature profile. The reason the ion temperature near the axis in NCLASS is relatively low may be attributed to the strong influence of the neoclassical thermal diffusivity whose

value is almost double in comparison with others.

5. In the case of the reversed shear configuration

We also make a comparison in the reversed shear configuration. The plasma parameters and conditions are the same as those of the high β_p mode. We show the results of the NCLASS model. The plasma current I_p is kept constant 1 MA for the first 1 s, then ramped up to 3 MA during the next 1 s, and kept to 3 MA for the last 1 s. The on-axis heating of 10 MW is switched on at the beginning of the current ramp up.

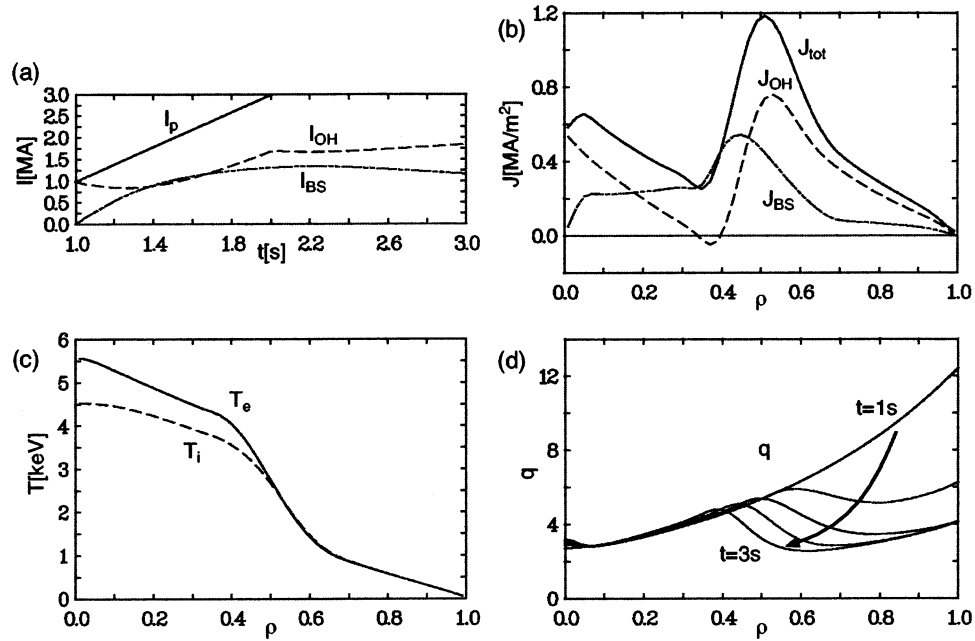


Fig. 4 (a) Time evolution of the plasma current, and radial profiles of (b) the current density, (c) the electron and ion temperature at $t = 3$ s and (d) the safety factor including a time evolution in the reversed shear configuration.

The plasma profiles at $t = 3$ s and the time evolution are shown in Fig. 4. It is clear that the position of the ITB shoulder in Fig. 4(c) corresponds to that of the peak of the bootstrap current J_{BS} near $\rho = 0.4$ in Fig. 4(b) and the position of the ITB foot corresponds to that of the bottom of the safety factor q near $\rho = 0.6$ in Fig. 4(a). The current ramping up and the heating cause an increase of the bootstrap fraction $f_{BS} \sim 0.4$ shown in Fig. 4(a). Accordingly, it results in the hollow shaped q profile, which produces the negative shear. Therefore the negative shear s and steep pressure gradient α would suppress the turbulence and lead to the reduction of the thermal diffusivity. The above-mentioned factors would be important for the formation of a strong ITB in the reversed shear configuration.

In comparison with previous calculations with Hinton, Hazeltine model, the magnitude of the bootstrap current with NCLASS is larger and the profile is broader. The magnitude of the safety factor is globally larger. On the other hand, the neoclassical thermal diffusivity near the axis is also notably larger.

6. Conclusion

We made a comparison amongst the four bootstrap current models, and we found that the neoclassical resistivity is similar to each other, but the bootstrap current profile has large divergence and the relation of the magnitude, $J_{NCL} > J_{Sau} > J_{H\&H} > J_{Wil}$, usually holds.

In the high β_p mode, each model enabled us to reproduce the ITB at the same position, but the ion temperature in the case of NCLASS was lower because of the large neoclassical ion thermal diffusivity. Using NCLASS, we also reproduced the formation of the strong ITB in the reversed shear configuration.

Reference

- [1] K. Itoh *et al.*, Plasma Phys. Control. Fusion **35**, 543 (1993).
- [2] A. Fukuyama *et al.*, Plasma Phys. Control. Fusion **37**, 543 (1995).
- [3] W.A. Houlberg *et al.*, Phys. Plasmas **4**, 3230 (1997).
- [4] O. Sauter *et al.*, Phys. Plasmas **6**, 2834 (1999).
- [5] F.L. Hinton and R.D. Hazeltine, Rev. Mod. Phys. **48**, 239 (1976).
- [6] J. Wesson, *Tokamaks second edition* (CLARENDON PRESS, 1997).
- [7] S.P. Hirshman, R.J. Hawryluk and B. Birge, Nucl. Fusion **17**, 611 (1977).